JACS
JOURNAL OF THE AMERICAN CHEMICAL SOCIETY
Article
pubs.acs.org/JACS

Stabilizing Structure-Switching Signaling RNA Aptamers by Entrapment in Sol–Gel Derived Materials for Solid-Phase Assays

Carmen Carrasquilla,[†] Pui Sai Lau,[‡] Yingfu Li,[†,‡] and John D. Brennan*[,†]

[†]Department of Chemistry and Chemical Biology, McMaster University, Hamilton, Ontario, Canada, L8S 4M1
[‡]Department of Biochemistry and Biomedical Sciences, McMaster University, Hamilton, Ontario, Canada, L8N 3Z5

Supporting Information

ABSTRACT: Structure-switching, fluorescence-signaling DNA and RNA aptamers have been reported as highly versatile molecular recognition elements for biosensor development. While structure-switching DNA aptamers have been utilized for solid-phase sensing, equivalent RNA aptamers have yet to be successfully utilized in solid-phase sensors due to their lack of chemical stability and susceptibility to nuclease attack. In this study, we examined entrapment into sol–gel derived organic–inorganic composite materials as a platform for immobilization of structure-switching fluorescence-signaling RNA aptamer reporters, using both the synthetic theophylline- and naturally occurring thiamine pyrophosphate-binding RNA aptamers as test cases. Structure-switching versions of both aptamers were entrapped into a series of sol–gel derived composites, ranging from highly polar silica to hydrophobic methylsilsesquioxane-based materials, and the target-binding and signaling capabilities of these immobilized aptamers were assessed relative to solution. Both immobilized aptamers demonstrated sensitivity and selectivity similar to that of free aptamers when entrapped in a composite material derived from 40% (v/v) methyltrimethoxysilane/tetramethoxysilane. Importantly, this material also conferred protection from nuclease degradation and imparted long-term chemical stability to the RNA reporter systems. Given the versatility of sol–gel entrapment for development of biosensors, microarrays, bioaffinity columns, and other devices, this entrapment method should provide a useful platform for numerous solid-phase RNA aptamer-based devices.

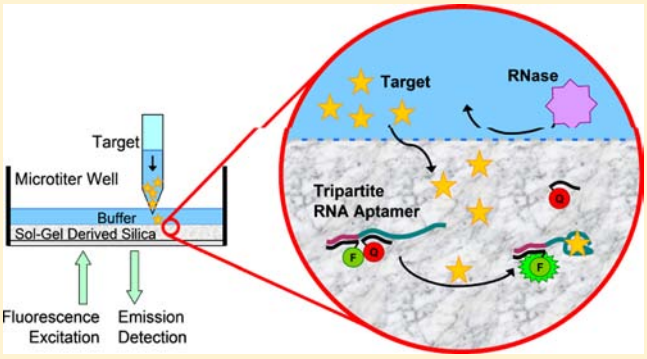

INTRODUCTION

Aptamers are single-stranded nucleic acids commonly generated through *in vitro* selection that can function as receptors for small molecules, proteins, or even cells, due to their ability to fold into distinct three-dimensional structures[1−3] that possess specificity and affinity for their target ligands comparable to, if not surpassing, that of antibodies.[4] These features, combined with their chemical stability and ease of modification, have seen DNA aptamers emerge as promising biological recognition elements in analytical and diagnostic applications.[5−9] However, the limited range of analytes for DNA aptamers (with only 12 small-molecule and 9 protein targets as of 2009)[10] and the lack of known naturally evolved DNA aptamers limit their potential for widespread use in sensing applications.

RNA aptamers, by contrast, can fold into more complex structures in order to provide a greater diversity of potential analytes as demonstrated by over 90 unique RNA aptamers for various small-molecule and protein targets.[10−12] Moreover, RNA aptamers have recently been derived from natural sources (i.e., riboswitches).[13−15] However, reports on the use of RNA-based aptamers in solution or solid-phase biosensing applications are still relatively limited, mostly due to their inherent chemical instability[16−18] and susceptibility to nuclease attack,[19] combined with their lack of intrinsic signal-development capabilities. Several studies have focused on increasing the stability of functional RNA, usually by substituting the highly reactive hydroxyl group at the 2′-position of nucleotides containing pyrimidines, to make them nuclease-resistant.[20−24] However, chemical modification of RNA aptamers may alter their selectivity and binding affinity[25] without a significant increase in stability if the aptamer is purine rich. Studies involving *in vitro* selections using a combinatorial library with modified bases[26] or Spiegelmers[27−29] (mirror-image nucleotides) have generated families of aptamers with distinctly dissimilar minimal sequences compared to conventional RNA aptamers, providing completely different molecules and making these methods of limited use for unmodified RNA aptamers that are naturally occurring or have already been selected in the past twenty years.

Recently, the Li group addressed the signaling ability of RNA aptamers by developing a structure-switching/fluorescence-signaling approach similar to that described previously for DNA

Received: April 27, 2012
Published: June 22, 2012

aptamers.[30] The synthetic theophylline-binding aptamer (33 nt, 100 nM K_d)[31] and the naturally occurring thiamine pyrophosphate (TPP)-binding aptamer (87 nt, 0.85 nM K_d)[32] were converted to reporter systems by designing complementary fluorophore-labeled DNA (FDNA) and quencher-labeled DNA (QDNA) strands to assemble a tripartite signaling duplex such that a conformational change from a RNA/DNA duplex to a RNA/target complex was coupled to a fluorescence-dequenching mechanism, generating a fluorescence signal upon target binding (secondary structures of both reporters are provided in the Supporting Information, Figure S1). While the structure-switching reporters retained the same specificity as the original aptamers, the affinities of both aptamers were observed to be ~10-fold poorer than the original K_d values (1 and 0.1 μM, respectively), with maximal signal enhancements of ~6-fold and 3.5-fold for the theophylline-binding and TPP-binding aptamer, respectively.[33]

To extend the utility of signaling RNA aptamers for diagnostic applications, it is generally necessary to immobilize these species onto or within a suitable surface while maintaining chemical stability and structure-switching abilities.[34] At this time, very few studies have examined immobilized RNA aptamers for solid-phase biosensing devices,[35−41] and none have examined the immobilization of structure-switching signaling RNA aptamers. In this report, we investigate the use of a low temperature sol−gel process for entrapment of structure-switching RNA aptamers into porous silica and organosilane materials.[42,43] This simple immobilization process has been shown to be "biofriendly" and applicable to the entrapment of a variety of viable biomolecules,[44−49] including structure-switching DNA aptamers[50] and DNA enzymes,[51] suggesting that the method should be useful for the development of solid-phase RNA aptamer biosensors. However, the entrapment of functional RNA aptamers requires a material that can stabilize these labile molecules against degradation by both intramolecular transesterification and external nuclease attack. Therefore, structure switching variants of both an *in vitro* selected RNA aptamer and a naturally occurring aptamer were entrapped in a variety of sol−gel processed composite materials (polar, anioinic, cationic, hydrophobic) and the leaching, chemical stability, resistance to nuclease attack and signaling capabilities were evaluated relative to these species in solution. The data clearly show that the optimal materials for entrapment of RNA aptamers are very different from those that stabilize proteins, and demonstrate the versatility of the sol−gel immobilization method to expand solid-phase sensing through the utilization of relatively unexplored RNA aptamer species.

RESULTS AND DISCUSSION

Characterization of Sol−Gel Derived Materials. Sol−gel derived materials were prepared from two previously reported biofriendly precursors (sodium silicate (SS) and diglyceryl silane (DGS)) with and without 3-aminopropyltriethoxysilane (APTES) (to produce a cationic surface), along with tetramethylorthosilicate (TMOS) derived composites containing up to 80% methyltrimethoxysilane (MTMS) to produce a gradient of polarity, and methylsilsesquioxane (MSQ) materials derived from pure MTMS to examine whether aptamers could be entrapped into highly hydrophobic materials. Prior to performing studies focused on the leaching of tripartite RNA aptamers from the various sol−gel materials, the polarity (as judged by contact angle) and morphology of all materials were assessed. The data (Table S1, Supporting Information) showed that all silica-based materials, with or without added APTES, had contact angles in the range of 16−28°, indicative of highly polar, hydrophilic materials. Addition of MTMS caused a nonlinear increase in contact angle, with only moderate increases in contact angle up to 40% MTMS (49°), followed by a large increase in contact angle to 91° at 60% MTMS and 120° for MSQ, indicative of a highly hydrophobic material. The morphology of the materials was also highly dependent on composition, with high surface areas and namometer scale pores, indicative of mesoporous materials, being observed up to 60% MTMS, followed by a sudden change to low surface area macroporous materials at 80% MTMS and above (see scanning electron microscopy images of all materials in Supporting Information, Table S2). These data show that the switchover from predominantly silica to predominantly MSQ-based materials resulted in a loss of mesopores and a tendency toward phase separation to generate macropores.[42]

Leaching of Aptamers from Sol−Gel Derived Materials. The extent of leaching of the entrapped aptamer was evaluated for each material, as indicated in Figure 1. Leaching

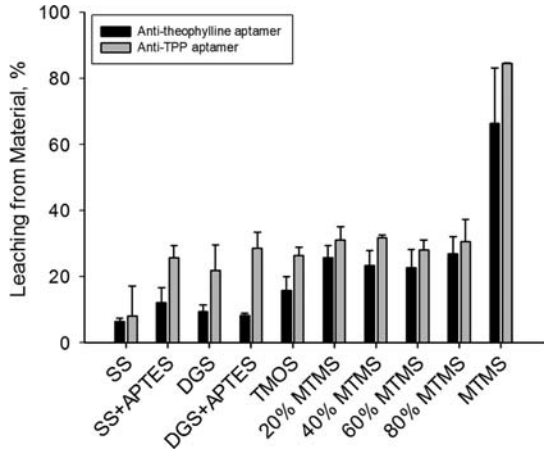

Figure 1. Leaching of the antitheophylline and anti-TPP RNA aptamer reporter constructs from various sol−gel derived materials.

ranged from a low of ~5% in SS materials to ~30% in materials containing up to 80% MTMS, and then increased to 60−80% in pure MSQ materials, depending on the aptamer, demonstrating the general trend of increased leaching with increased hydrophobicity and increased pore size. Leaching was generally higher for the anti-TPP aptamer relative to the antitheophylline aptamer, and typically occurred predominantly during the first washing step. The very large extent leaching in pure MSQ materials is likely reflective of the lack of mesopores, which would be expected to retain the small aptamers while macropores would not. The MSQ materials also are unlikely to be able to template around the RNA aptamers to aid in retention, as has been reported for some proteins entrapped in silica.[51]

The overall degree of leaching is relatively high compared proteins, but is similar to that of DNA aptamers entrapped in polar silica monoliths.[50] This previous study found that the attachment of a bulky streptavidin protein to biotinylated DNA, used to enlarge the molecular complex, did not improve leaching within error. Use of steptavidin would also be incompatible with the use of hydrophobic composites, and

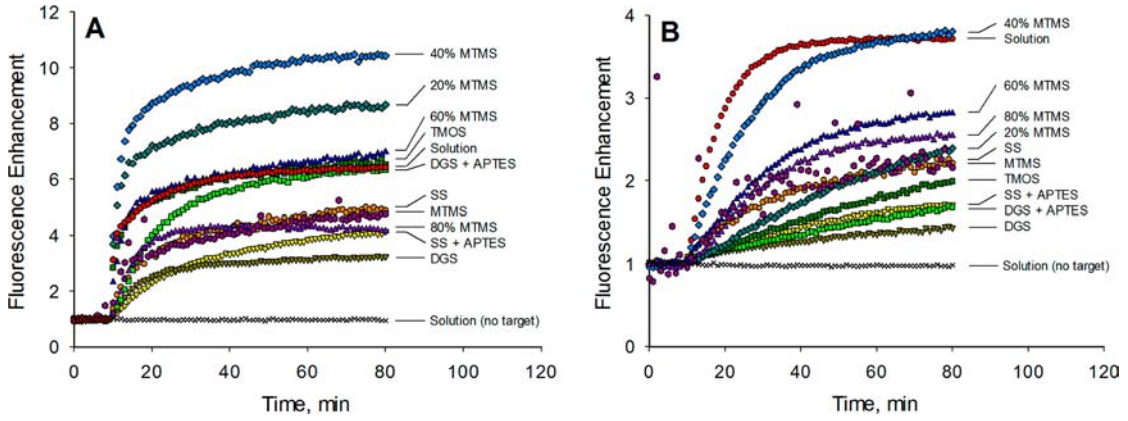

Figure 2. Fluorescence signaling ability of RNA aptamer reporters in solution and in various sol–gel derived materials. Target-induced response of the (A) theophylline-binding aptamer and (B) TPP-binding aptamer upon exposure to 1 mM theophylline and 100 μM TPP, respectively, after 10 min baseline incubation.

thus this strategy was not examined in this study. Since fluorescence intensity measurements are used to determine the amount of leaching, the FDNA cannot be distinguished from the FDNA-aptamer complex. However, given that the FDNA is essential for signaling target binding in the tripartite design, measuring leaching of these short 20-nt oligonucleotide components is of equal importance for this reporter system.

Signal Generation from Entrapped RNA Aptamer Reporters. A key requirement for entrapped structure-switching signaling aptamers is the ability to undergo conformational changes upon binding of ligands and to subsequently release the QDNA strand to elicit a fluorescence response. Experiments were performed to assess the degree of signal enhancement upon target binding for each RNA aptamer entrapped in the full series of sol–gel derived materials. All materials were first washed to remove leachable aptamers, followed by addition of either 1 mM theophylline or 100 μM TPP to the appropriate RNA reporter system. Figure 2 shows relative fluorescence enhancement and rate of signal development for each of the RNA aptamers when in solution and entrapped in the various sol–gel derived materials. Consistent with the previous findings,[33] full signal development required a longer time for the anti-TPP aptamer relative to the antitheophylline aptamer, even in solution. When entrapped, both aptamer reporter systems were able to structure-switch and produce a fluorescence signal in all materials; however, the signal enhancements and rates of signal development were highly dependent on the type of sol–gel derived material used for entrapment.

Composite materials derived from mixtures of MTMS and TMOS always produced higher signal enhancements than polar silica materials (SS, DGS) or nonpolar MSQ materials. Previous studies have shown that only a small fraction (~10%) of biomolecules entrapped in polar materials are inaccessible to external analytes,[50,52] thus the loss of signal in polar materials likely reflects electrostatic aptamer backbone-silica interactions that prevented structure switching of the aptamer. The high silica content of polar materials may also be detrimental to the chemical stability of RNA by promoting hydrolysis reactions, which cause cleavage of the phosphodiester linkages to degrade the aptamer.[16] DGS derived materials demonstrated the lowest enhancement for both aptamers, which is not surprising since it has been suggested that glycerol modifies electrostatic interactions between polynucleotides[53] and destabilizes double-stranded DNA.[54] Thus, this byproduct of DGS condensation, though proven as a stabilizer of proteins, appears to destabilize the double-stranded structure required for the intact RNA aptamer reporter complex, causing higher background fluorescence and a poorer signal enhancement. Interestingly, both reporters showed decreased signal enhancements when entrapped in SS +APTES (compared to SS materials) while the addition of APTES to DGS improved the signal generation, particularly for the antitheophylline aptamer. The inconsistent results related to the addition of APTES are not fully understood, but suggest that this species may be located in different environments in SS relative to DGS derived materials, or that the strength of its electrostatic effects differ in materials with varied porosity and pore size, as suggested by previous studies entrapping DNA in cationic hydrogels.[55] The low signal enhancement and high variability in pure MSQ materials is most likely due to the significant leaching of the reporters from this particular matrix.

The best overall performance for both aptamers (highest signal enhancement and fastest signal development) was observed using an organic–inorganic hybrid material composed of 40% MTMS and 60% TMOS (v/v), suggesting that this material had the best balance of polarity and surface charge that minimized analyte- and/or RNA-surface interactions while retaining enough conformational flexibility to allow for structure-switching and signaling to occur. When compared to the signal enhancement obtained in solution, the entrapped theophylline-binding RNA generated a greater enhancement, up to 10-fold as compared to 6-fold in solution. The signal enhancement of the TPP-binding aptamer was comparable to that of the solution, with almost a 4-fold enhancement. The high signal enhancements observed for both aptamers using this material may also be due to alterations in the local pH of the microenvironment around the aptamers (see below) or restriction of RNA backbone mobility caused by entrapment in the pores of a partially hydrophobic composite matrix.

The physical restriction of RNA mobility appears to stabilize the secondary structure of the entrapped RNA aptamers, promoting FDNA/QDNA hybridization for a lower background signal and preventing sampling of in-line geometries that induce intramolecular cleavage.[18] These effects would be more evident using the smaller theophylline-binding aptamer, which has a larger amount of its sequence hybridized to DNA and a shorter flexible single-stranded region that is less likely to

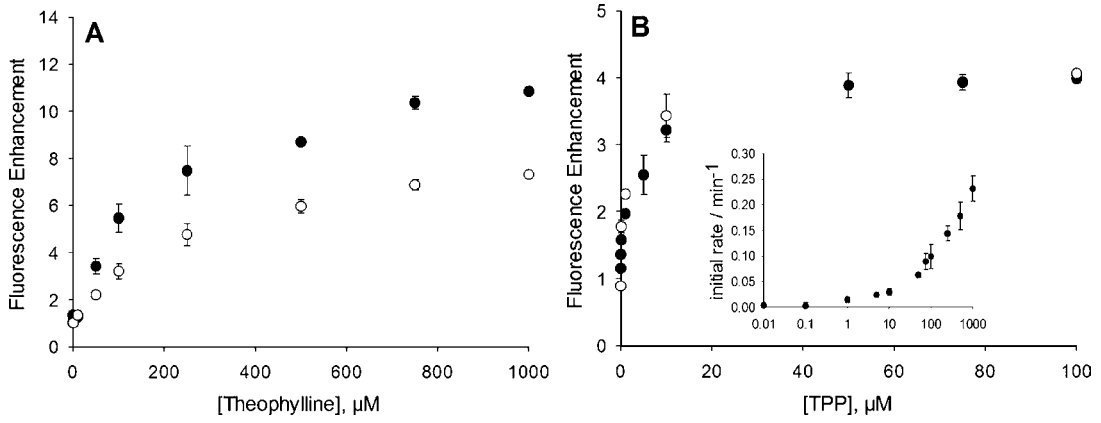

Figure 3. Sensitivity of the sol–gel entrapped RNA aptamer reporters. Response curve of the (A) theophylline-binding aptamer to increasing theophylline concentrations and (B) TPP-binding aptamer to increasing TPP concentrations, either entrapped in the 40% MTMS material (●) or in solution (○). (Inset of B) Change in initial signaling rate of the entrapped TPP-binding aptamer when exposed to increasing TPP concentrations.

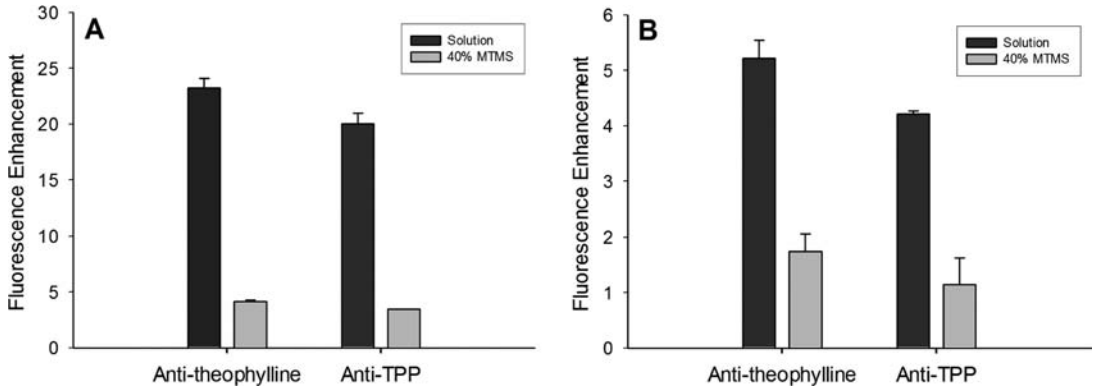

Figure 4. Changes in emission intensity of RNA aptamer reporters upon exposure to RNase A or RNase H. Fluorescence measurements 2 h after addition of 3 units of (A) RNase A or (B) RNase H to the theophylline-binding and TPP-binding reporter constructs in solution or entrapped within the sol–gel derived material.

sample conformations susceptible to spontaneous cleavage, producing the significant improvement in signaling that was observed for this particular aptamer.

Sensitivity and Selectivity of Entrapped RNA Aptamer Reporters. Figure 3A and B shows the target concentration-dependent signal enhancements of the antitheophylline and anti-TPP aptamers, respectively, when entrapped in the 40% MTMS material and in solution. The antitheophylline RNA reporter demonstrated a similar detection limit and dynamic range to that reported in solution (1–1000 μM) while the anti-TPP aptamer had a detection limit of 1 μM, which was 10-fold worse than the value in solution, and a dynamic range up to 100 μM, which was similar to the value in solution.[33] The poorer detection limit may be due to the exclusion of the anionic TPP from the hydrophobic matrix, which would require a higher external concentration to reach a sufficient internal concentration to produce signaling. Interestingly, the use of initial rate data provided a broader dynamic range for TPP sensing while maintaining the detection limit of 1 μM (Figure 3B, inset).

The selectivity of entrapped RNA reporters was assessed using molecules that were chemically similar to their targets. These included caffeine and theobromine for the theophylline-binding aptamer and thiamine monophosphate (TMP), thiamine and oxythiamine for the TPP-binding aptamer. Mutant versions of each RNA aptamer were also entrapped and subjected to either theophylline or TPP at concentrations of 1 mM and 100 μM, respectively. Selectivity was maintained for both entrapped aptamer reporters, with little to no change in responses when using structural derivatives of targets or mutant constructs (Supporting Information, Figure S2).

RNA Aptamer Sensitivity to Ribonucleases. Previous studies have shown that entrapping DNA aptamers within a polyacrylamide hydrogel[56] or silica matrix[50] can provide a steric barrier to digestive enzymes, such as DNase I. To assess the protective effects of entrapment in MTMS/TMOS composites on the RNA reporters, the stability of free (solution) and entrapped aptamers toward digestion by two different ribonucleases was compared. RNase A was chosen since it is abundant in biological fluids and is pyrimidine-specific,[57] while RNase H is known to degrade the RNA from RNA/DNA hybrids[58] such as the tripartite reporter complex in this work. Degradation by either ribonuclease can be monitored by an increase in fluorescence as the distance between the fluorescein and dabcyl moieties increases due to release of the QDNA, FDNA or both from the digested RNA aptamer strand. As shown in Figure 4, the addition of RNase A or RNase H to either RNA aptamer reporter in solution resulted in an increase in fluorescence of greater than 20-fold and 4-fold, respectively. In the case of the aptamers entrapped in the 40% MTMS sol–gel derived material, less than 4-fold and 2-fold fluorescence enhancements were observed upon addition of RNase A or RNase H, respectively. These results indicate that both ribonucleases are unable to enter the material and access the entrapped RNA aptamers, producing 80% less digestion with

dx.doi.org/10.1021/ja304064a | J. Am. Chem. Soc. 2012, 134, 10998–11005

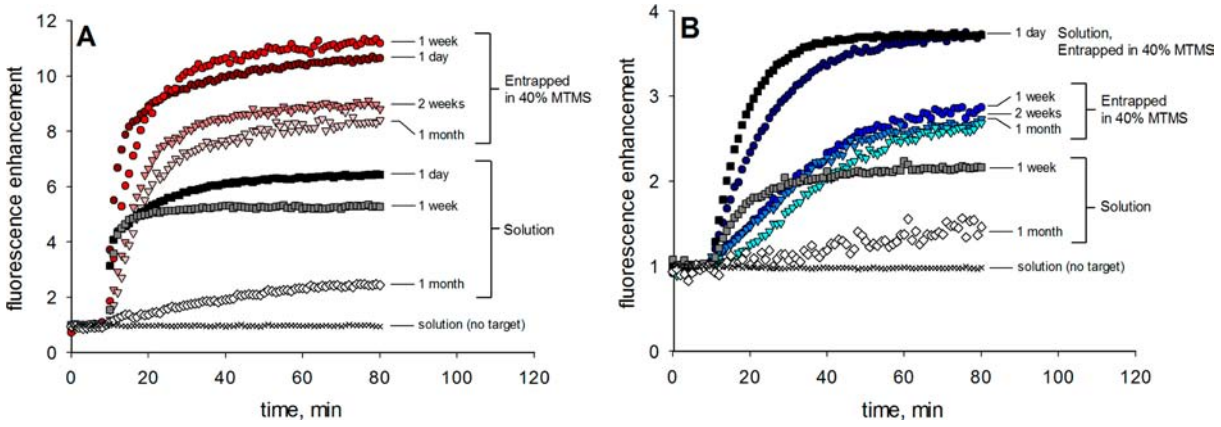

Figure 5. Structure-switching and signaling ability of RNA aptamer reporters after different storage time. Target-induced fluorescence signaling ability of solution-based or entrapped RNA aptamer reporters after increasing storage time at 4 °C of the (A) theophylline-binding aptamer using 1 mM theophylline and (B) TPP-binding aptamer using 100 μM TPP, after 10 min baseline incubation.

RNase A and 70% less digestion when using RNase H. The small amount of degradation is likely due to the digestion of aptamer molecules that reside very close to the surface of the small silica disks (less than 1 mm thickness). These thin monoliths have a much higher surface area-to-volume ratio than typical large bulk monoliths, but are more representative of a biosensor design that uses thin films to minimize target diffusion time. Overall, these results indicate that the majority of the entrapped RNA was not accessible to the RNase enzymes and thus was well-protected from digestion when entrapped in the mesoporous matrix.

Effects of Long-term Storage on RNA Aptamer Activity. The long-term stability of the RNA reporters was examined when entrapped in the 40% MTMS material and compared to RNA reporters in solution. Figure 5 demonstrates that, when in solution, the activity of the theophylline-binding aptamer after 1 week is similar to the level in a freshly prepared solution, while that of the 1 week old TPP-binding aptamer is almost half the original activity. This is consistent with the hypothesis that the larger anti-TPP aptamer undergoes greater intrinsic cleavage due to in-line nucleophilic attack. However, after 1 month of storage in solution, both RNA aptamer reporters show relatively low signal enhancements upon target addition with about 2-fold increase for the antitheophylline aptamer and 1.5-fold enhancement with the anti-TPP aptamer. This loss in signal is due to higher fluorescence backgrounds as the RNA is degraded over time, causing release of the fluorescent moiety from its close interaction with the quencher prior to introduction of the target.

When the aptamers were entrapped in the 40% MTMS/60% TMOS derived material and then stored up to 1 month, the signal enhancements were maintained above 8-fold and 2.5-fold for the theophylline-binding and TPP-binding aptamers, respectively. The observed loss of activity (~20−30%) likely reflects continued evolution of the sol−gel matrix, which could lead to pore shrinkage and subsequent restriction of dynamic motion or restriction of access of anlaytes to the entrapped RNA[42,59] (currently under investigation). Initial fluorescence levels of all aged materials (1 week to 1 month) were slightly lower than those of newly prepared composites, indicating that the entrapped aptamers were not being degraded upon storage, although further leaching of surface-proximal RNA during the longer storage periods may have contributed to the observed loss in activity (fluorescence intensity values provided in Table S3 of Supporting Information). The ability to remove leached FDNA or degraded aptamer as a means of lowering background signals highlights another benefit of entrapment over solution-based studies. In general, although the signal enhancements of both aptamers are slightly reduced over the first 1−2 weeks, the signaling ability is maintained over an extended storage time, highlighting the ability of the matrix to protect the RNA aptamers from both intrinsic chemical instability and external enzymatic degradation, and leading to a more robust solid-phase sensor.

The origin of the enhanced chemical stability is not fully understood at this time. However, it is well-known that under neutral or alkaline pH conditions (in the presence of alkali metals and alkali-earth metals), the dominant pathway for RNA chemical degradation is the internal phosphoester transfer reaction via an SN2 mechanism wherein the 2′-oxygen attacks the adjacent phosphorus center.[16] The protonation state of the 2′-oxygen largely dictates this rate of transesterification, which is enhanced by specific base catalysis through deprotonation of the 2′-hydroxyl group to the more nucleophilic 2′-oxyanion group.[17] Thus, in solution, exposure to hydroxide ions increases the fraction of these reactive 2′-oxyanion groups to promote RNA cleavage. However, when entrapped in a relatively hydrophobic sol−gel derived matrix, the RNA species interacts with only a few hydroxide ions present in the thin solution layer between the biomolecule and the material surface,[60] effectively decreasing the hydroxide-dependent degradation rate. Moreover, previous studies[61] have shown that the apparent pK_a of pH sensitive dyes increases when entrapped in organic−inorganic composites, demonstrating that the effective pH within the composites is less basic that in the surrounding solution (i.e., a probe with a pK_a of 6.0 in solution has an apparent pK_a of 8.3 in materials composed of MTES/TEOS). Additional studies are currently underway to further examine the specific effects of entrapment in inorganic materials that chemically stabilize RNA.

■ CONCLUSIONS

A simple and general approach for improving the stability of RNA aptamers is demonstrated based on their entrapment in a sol−gel derived composite material. Two different RNA aptamer reporters retained maximum sensitivity and selectivity when entrapped in an organic−inorganic composite material prepared by cohydrolysis and condensation of 40% MTMS and

60% TMOS (v/v). Since the RNA reporter system was entrapped in the pores of the sol–gel derived matrix, it was relatively well protected from nuclease degradation and, perhaps more importantly, the composite material also reduced the extent of in-line chemical degradation, providing the long-term stability required of a robust biosensor. As such, this immobilization scheme expands the use of functional nucleic acids from the limited number of DNA aptamers to the much broader range of relatively unexplored RNA aptamer species.

Importantly, sol–gel derived materials possess significant versatility in that they are amenable to many configurations, including microarrays, bioaffinity columns or thin-film coatings for interfacing to various analytical devices.[43,62] Although the current study focuses on fluorescence signaling in monolithic materials, the use of the sol–gel method for biomolecular entrapment has been utilized in both colorimetric and electrochemical sensors[63] and thus presents a broadly applicable platform for preparing solid-phase RNA aptamer sensors. Such biosensors may find wide appeal in environmental and clinical analysis, particularly for the detection of small metabolites, an area where elicitation of monoclonal antibodies is difficult.

EXPERIMENTAL SECTION

Chemicals. All DNA oligonucleotides were synthesized using standard phosphoramidite chemistry by Integrated DNA Technologies (Coralville, IA) and purified by 10% denaturing PAGE prior to use. Fluorescently labeled DNA oligonucleotides were purified by HPLC as described elsewhere.[30] Theophylline, theobromine, caffeine, thiamine pyrophosphate (TPP), thiamine monophosphate (TMP), thiamine, oxythiamine, tetramethylorthosilicate (TMOS), methyltrimethoxysilane (MTMS), 3-(aminopropyl)triethoxysilane (APTES) and Dowex 50 × 8–100 cation exchange resin were obtained from Sigma-Aldrich (Oakville, ON). Ribonuclease A (RNase A) and ribonuclease H (RNase H) were purchased from Fermentas Life Sciences (Burlington, ON). Sodium silicate solution (SS solution, ultrapure grade, ~14% Na_2O, ~29% silica) was purchased from Fisher Scientific (Pittsburgh, PA). Diglycerylsilane (DGS) was prepared from TMOS as described elsewhere.[64,65] Water was purified with a Milli-Q Synthesis A10 water purification system and autoclaved. Buffer salt solutions were autoclaved after preparation and all other chemicals and solvents were of analytical grade and were used as received.

Preparation of RNA Aptamers and Reporter Constructs. Polymerase chain reaction of the DNA templates for the theophylline and TPP aptamer, as well as RNA transcription of these RNA aptamers, was performed as described elsewhere.[33] The specific DNA template sequences used in this work were as follows.

DNA template for the theophylline reporter: 5′-GAATT CTAAT ACGAC TCACT ATAGG CCTGC CACGC TCCGA CGCTA TCACT CTATG GGCGA TACCA GCCGA AAGGC CCTTG GCAGC GTCCA ACACA TCG-3′ (in the mutant **1** template, C_{64} and A_{83} were mutated to A_{64} and T_{83}; in the mutant **2** template, $C_{63}C_{64}$ were replaced with $G_{63}A_{64}$).

Theophylline aptamer template forward primer: 5′-GAATT CTAAT ACGAC TCACT ATA-3′.

Theophylline aptamer template reverse primer: 5′-CGATG TGTTG GACGC-3′.

DNA template for the TPP reporter: 5′-GAATT CTAAT ACGAC TCACT ATAGG CCTGC CACGC TCCGA CGCTA TCACT CTATG CCACT AGGGG TGCTT GTTGT GCTGA GAGAG GAATA ATCCT TAACC CTTAT AACAC CTGAT CTAGG TAATA CTAGC GAAGG GAAGT GG-3′ (mutant **1** template was made by replacing G_{60}, G_{74}, G_{76}, A_{77} and G_{126} with C_{60}, C_{74}, T_{66}, T_{67}, T_{126}, while in the mutant **2** template, G_{60}, T_{73},G_{74}, G_{76}, A_{77}, C_{125}, G_{126}, G_{131}, A_{132} were mutated to C_{60}, C_{73}, C_{74}, T_{66},T_{67}, A_{125}, T_{126}, C_{131}, G_{132}).

TPP aptamer template forward primer: 5′-GAATT CTAAT ACGAC TCACT ATA-3′.

TPP aptamer template reverse primer: 5′-GCTTC TGTTC CCACT-3′.

The tripartite complexes of these RNA aptamer reporters were prepared by combining 80 nM of the extended RNA aptamer with 40 nM of FDNA and 120 nM of QDNA in 50 mM Tris·HCl (pH 7.5) with 20 mM $MgCl_2$. This mixture was first heated at 65 °C for 2 min, cooled at room temperature for 10 min, and then stored at 4 °C until analysis. The sequences of the fluorescein-labeled (FDNA) and DABCYL-labeled (QDNA) oligonucleotides were as follows.

Theophylline/TPP aptamer FDNA: 5′-**F**TAGCG TCGGA GCGTG GCAGG-3′.

Theophylline aptamer QDNA: 5′-TATCG CCCAT AGAGT G**Q**-3′.

TPP aptamer QDNA: 5′-CTAGT GGCAT AGAGT G**Q**-3′.

Entrapment of Aptamers within Sol–Gel Derived Materials. Silane and organosilane precursors were used to prepare the sols for aptamer entrapment studies, including SS, DGS, TMOS, APTES and MTMS. Sodium silicate sols were prepared as described elsewhere[66] by diluting 2.6 g of a stock SS solution to 10 mL with water, mixing the solution with 5.5 g of DOWEX to bring the pH of the SS solution to ~4, and then filtering this solution through a Büchner funnel to remove the resin followed by further filtration through a 0.45 μM membrane syringe filter to remove any particulates in the solution. The DGS precursor sol was prepared by grinding DGS to a fine powder and dissolving 0.5 g in 1 mL of water, followed by 15 min sonication in ice-cold water and filtering the solution through a 0.2 μM membrane syringe filter. Materials containing 0.1% (v/v) APTES in either SS or DGS were also tested, with the APTES added to the sol prior to addition of aptamer solutions. To make TMOS and MTMS sols, 700 μL of water and 50 μL of HCl (0.1 N) were added to 2.25 mL TMOS or MTMS and then sonicated for 20 min in ice-cold water as described elsewhere.[51] The TMOS-MTMS mixtures were prepared by proportionally dividing the 2.25 mL of silane using volume percentages of 20–80% MTMS in TMOS, mixing with water and acid and cohydrolyzing in a sonicator as described above.

Tripartite aptamer complexes (in a 1:2:3 FDNA/RNA/QDNA molar ratio) for entrapment were prepared at double the concentration of typical solutions in 100 mM Tris·HCl (pH 7.5) with 40 mM $MgCl_2$ and heated at 65 °C for 2 min, cooled at room temperature for 10 min, then stored at 4 °C until mixing in a 1:1 volume ratio with a freshly prepared silica sol at room temperature. The aptamer-sol mixtures were deposited into 96-well microtiter plates at a volume of 50 μL per well and allowed to gel. These plates were then left to age at 4 °C for at least 4 h and then overlaid with 100 μL of 50 mM Tris·HCl (pH 7.5) with 20 mM $MgCl_2$ prior to washing and analysis.

Characterization of Sol–Gel Derived Silica Morphology. Larger monoliths (3 mL total volume of 1:1 sol–gel precursor/buffer, v/v) of the various sol–gel derived materials described above were prepared without entrapped aptamer. After gelation, all monoliths were cured in air for 4–6 h at 20 °C prior to aging for 5 days in sealed vials. Water contact angle measurements were performed using a Krüss drop shape analyzer system (DSA10, Dataphysics) at 25 °C by applying conventional sessile drops on the material surface. Average contact angle was calculated from three values obtained from different areas of each sample. These monoliths were then desiccated for another 7 days, crushed and outgassed for 8–12 h to remove air and residual water from the surface prior to performing porosimetry measurements. Nitrogen porosimetry and mercury intrusion analyses were carried out as described in detail elsewhere.[67] Samples for SEM imaging were aged for 10 days before analysis and coated with 5 nm of platinum under vacuum to improve conductivity. Imaging was performed at 5 kV using a JEOL JSM 7000F Scanning Electron Microscope.

Leaching Studies. Prior to any fluorescence measurements, the various sol–gel derived materials containing the reporter complexes were washed three times with 100 μL buffer at room temperature to remove any unencapsulated RNA from the material surface. Leaching

of entrapped aptamers from the materials was determined by comparing the total fluorescence intensity prior to any washing to that of washed materials, as well as the fluorescence intensity of the wash solutions for all three washes.

Target-binding Assays. All fluorescence assays were performed at 37 °C using a Tecan M1000 platereader. Both solution and sol–gel entrapped aptamer samples were excited at 490 nm and emission was collected at 520 nm using a 5 nm bandpass for both excitation and emission with a 0.5 s integration time using the bottom-read setting. Analytes (3 μL at the appropriate concentration) were either added directly to solution samples or the overlaying buffer of material samples after measuring initial baseline fluorescence for 10 min (stock analyte solutions were heated at 90 °C for 5 min and cooled to room temperature for 10 min prior to addition to ensure no contaminant RNase was introduced). Fluorescence emission was measured every 1 min for both baseline measurements and after target addition for a total of 80 min. Samples were corrected for light scattering by blank subtraction of signals originating from the materials or buffer without RNA reporters present. All fluorescence measurements are reported as fluorescence enhancement or F/F_o where F is the end point fluorescence intensity and F_o is the initial fluorescence intensity prior to target addition. Time-dependent measurements are represented by the average values of three independent experiments (with less than 10% variability), while error bars indicate the standard deviation of three independent experiments in end point bar graphs.

RNase Protection Assays. Either three (Kunitz) units of RNase A or three units of RNase H was added directly to solution samples or the overlaying buffer of material samples after measuring initial baseline fluorescence for 10 min, and fluorescence emission was measured every 1 min for 120 min using the same settings as were used for the target-binding fluorescence measurements.

Storage Stability Studies. The 40% MTMS materials containing the tripartite aptamer complexes were prepared and aged as described above. These materials were overlaid with 150 μL buffer and the microwell plates were covered with lids and wrapped in Parafilm to prevent evaporation upon storage. Plates were stored for 1 week, 2 weeks or 1 month at 4 °C in the dark prior to target-binding measurements and were compared to materials that had been aged for 1 day. Solutions containing the tripartite aptamer complexes were prepared in microcentrifuge tubes and stored for up to 1 month at 4 °C prior to target-binding measurements. No RNase inhibitors were used in this study.

■ ASSOCIATED CONTENT

Supporting Information

Physical characterization of the sol–gel derived materials, secondary structure of the RNA aptamer reporters, selectivity data of the entrapped RNA aptamer reporters, and supplementary fluorescence intensity data for storage stability studies. This material is available free of charge via the Internet at http://pubs.acs.org.

■ AUTHOR INFORMATION

Corresponding Author

brennanj@mcmaster.ca

Notes

The authors declare no competing financial interest.

■ ACKNOWLEDGMENTS

We thank the Natural Sciences and Engineering Research Council of Canada (NSERC) and the SENTINEL Bioactive Paper Network for funding this work. We also thank the Canada Foundation for Innovation and the Ontario Innovation Trust for support of this work. Y.L. holds the Canada Research Chair in Directed Evolution of Nucleic Acids. J.D.B. holds the Canada Research Chair in Bioanalytical Chemistry and Biointerfaces.

■ REFERENCES

(1) Wilson, D. S.; Szostak, J. W. *Annu. Rev. Biochem.* **1999**, *68*, 611–647.
(2) Ellington, A. D.; Szostak, J. W. *Nature* **1990**, *346*, 818–822.
(3) Tuerk, C.; Gold, L. *Science* **1990**, *249*, 505–510.
(4) Jayasena, S. D. *Clin. Chem.* **1999**, *45*, 1628–1650.
(5) Clark, S. L.; Remcho, V. T. *Electrophoresis* **2002**, *23*, 1335–1340.
(6) Hamula, C. L. A.; Guthrie, J. W.; Zhang, H.; Li, X.-F.; Le, X. C. *Trends Anal. Chem.* **2006**, *25*, 681–691.
(7) Song, S. P.; Wang, L. H.; Li, J.; Zhao, J. L.; Fan, C. H. *Trends Anal. Chem.* **2008**, *27*, 108–117.
(8) Sefah, K.; Phillips, J. A.; Xiong, X.; Meng, L.; Van Simaeys, D.; Chen, H.; Martin, J.; Tan, W. *Analyst* **2009**, *134*, 1765–1775.
(9) Liu, J.; Cao, Z.; Lu, Y. *Chem. Rev.* **2009**, *109*, 1948–1998.
(10) Silverman, S. K. In *Functional Nucleic Acids for Analytical Applications*; Li, Y., Yi, L., Eds.; Springer: New York, 2009; pp 47–108.
(11) Klug, S. J.; Famulok, M. *Mol. Biol. Rep.* **1994**, *20*, 97–107.
(12) Marshall, K. A.; Ellington, A. D. *Methods Enzymol.* **2000**, *318*, 193–214.
(13) Winkler, W. C.; Breaker, R. R. *ChemBioChem* **2003**, *4*, 1024–1032.
(14) Mandal, M.; Breaker, R. R. *Nat. Rev. Mol. Cell Biol.* **2004**, *5*, 451–463.
(15) Montange, R. K.; Batey, R. T. *Annu. Rev. Biophys.* **2008**, *37*, 117–133.
(16) Oivanen, M.; Kuusela, S.; Lonnberg, H. *Chem. Rev.* **1998**, *98*, 961–990.
(17) Li, Y.; Breaker, R. R. *J. Am. Chem. Soc.* **1999**, *121*, 5364–5372.
(18) Soukup, G. A.; Breaker, R. R. *RNA* **1999**, *5*, 1308–1325.
(19) Famulok, M.; Mayer, G.; Blind, M. *Acc. Chem. Res.* **2000**, *33*, 591–599.
(20) Pieken, W. A.; Olsen, D. B.; Benseler, F.; Aurup, H.; Eckstein, F. *Science* **1991**, *253*, 314–317.
(21) Cummins, L. L.; Owens, S. R.; Risen, L. M.; Lesnik, E. A.; Freier, S. M.; McGee, D.; Guinosso, C. J.; Cook, P. D. *Nucleic Acids Res.* **1995**, *23*, 2019–2024.
(22) Kubik, M. F.; Bell, C.; Fitzwater, T.; Watson, S. R.; Tasset, D. M. *J. Immunol.* **1997**, *159*, 259–267.
(23) Kujau, M. J.; Wolfl, S. *Nucleic Acids Res.* **1998**, *26*, 1851–1853.
(24) Kusser, W. *J. Biotechnol.* **2000**, *74*, 27–38.
(25) Jellinek, D.; Green, L. S.; Bell, C.; Lynott, C. K.; Gill, N.; Vargeese, C.; Kirschenheuter, G.; McGee, D. P.; Abesinghe, P.; Pieken, W. A. *Biochemistry* **1995**, *34*, 11363–11372.
(26) Burmeister, P. E.; Lewis, S. D.; Silva, R. F.; Preiss, J. R.; Horwitz, L. R.; Pendergrast, P. S.; McCauley, T. G.; Kurz, J. C.; Epstein, D. M.; Wilson, C.; Keefe, A. D. *Chem. Biol.* **2005**, *12*, 25–33.
(27) Klussmann, S.; Nolte, A.; Bald, R.; Erdmann, V. A.; Furste, J. P. *Nat. Biotechnol.* **1996**, *14*, 1112–1115.
(28) Leva, S.; Lichte, A.; Burmeister, J.; Muhn, P.; Jahnke, B.; Fesser, D.; Erfurth, J.; Burgstaller, P.; Klussmann, S. *Chem. Biol.* **2002**, *9*, 351–359.
(29) Eulberg, D.; Klussmann, S. *ChemBioChem* **2003**, *4*, 979–983.
(30) Nutiu, R.; Li, Y. *J. Am. Chem. Soc.* **2003**, *125*, 4771–4778.
(31) Jenison, R. D.; Gill, S. C.; Pardi, A.; Polisky, B. *Science* **1994**, *263*, 1425–1429.
(32) Welz, R.; Breaker, R. R. *RNA* **2007**, *13*, 573–582.
(33) Lau, P. S.; Coombes, B. K.; Li, Y. *Angew. Chem., Int. Ed.* **2010**, *49*, 7938–7942.
(34) Potyrailo, R. A.; Conrad, R. C.; Ellington, A. D.; Hieftje, G. M. *Anal. Chem.* **1998**, *70*, 3419–3425.
(35) Clark, S. L.; Remcho, V. T. *Anal. Chem.* **2003**, *75*, 5692–5696.
(36) McCauley, T. G.; Hamaguchi, N.; Stanton, M. *Anal. Biochem.* **2003**, *319*, 244–250.
(37) Minunni, M.; Tombelli, S.; Gullotto, A.; Luzi, E.; Mascini, M. *Biosens. Bioelectron.* **2004**, *20*, 1149–1156.

(38) Cho, E. J.; Collett, J. R.; Szafranska, A. E.; Ellington, A. D. *Anal. Chim. Acta* **2006**, *564*, 82−90.
(39) Min, K.; Cho, M.; Han, S. Y.; Shim, Y. B.; Ku, J.; Ban, C. *Biosens. Bioelectron.* **2008**, *23*, 1819−1824.
(40) Lee, H. S.; Kim, K. S.; Kim, C. J.; Hahn, S. K.; Jo, M. H. *Biosens. Bioelectron.* **2009**, *24*, 1801−1805.
(41) Ferapontova, E. E.; Olsen, E. M.; Gothelf, K. V. *J. Am. Chem. Soc.* **2008**, *130*, 4256−4258.
(42) Brinker, C. J.; Scherer, G. W. *Sol-Gel Science*; Academic Press: New York, 1990.
(43) Brennan, J. D. *Acc. Chem. Res.* **2007**, *40*, 827−835.
(44) O'Driscoll, K. F. *Methods Enzymol.* **1976**, *44*, 169−183.
(45) Avnir, D.; Braun, S.; Lev, O.; Ottolenghi, M. *Chem. Mater.* **1994**, *6*, 1605−1614.
(46) Braun, S.; Rappoport, S.; Zusman, R.; Avnir, D.; Ottolenghi, M. *Mater. Lett.* **1990**, *10*, 1−5.
(47) Bhatia, R. B.; Brinker, C. J.; Gupta, A. K.; Singh, A. K. *Chem. Mater.* **2000**, *12*, 2434−2441.
(48) Jin, W.; Brennan, J. D. *Anal. Chim. Acta* **2002**, *461*, 1−36.
(49) Pierre, A. C. *Biocatal. Biotransform.* **2004**, *22*, 145−170.
(50) Rupcich, N.; Nutiu, R.; Li, Y.; Brennan, J. D. *Anal. Chem.* **2005**, *77*, 4300−4307.
(51) Shen, Y. T.; Mackey, G.; Rupcich, N.; Gloster, D.; Chiuman, W.; Li, Y. F.; Brennan, J. D. *Anal. Chem.* **2007**, *79*, 3494−3503.
(52) Sui, X.; Cruz-Aguado, J. A.; Chen, Y.; Zhang, Z.; Brook, M. A.; Brennan, J. D. *Chem. Mater.* **2005**, *17*, 1174−1182.
(53) Del Vecchio, P.; Esposito, D.; Ricchi, L.; Barone, G. *Int. J. Biol. Macromol.* **1999**, *24*, 361−369.
(54) Bonner, G.; Klibanov, A. M. *Biotechnol. Bioeng.* **2000**, *68*, 339−344.
(55) Joseph, K. A.; Dave, N.; Liu, J. *ACS Appl. Mater. Interfaces* **2011**, *3*, 733−739.
(56) Dave, N.; Chan, M. Y.; Huang, P.-J. J.; Smith, B. D.; Liu, J. *J. Am. Chem. Soc.* **2010**, *132*, 12668−12673.
(57) Raines, R. T. *Chem. Rev.* **1998**, *98*, 1045−1066.
(58) Donis-Keller, H. *Nucleic Acids Res.* **1979**, *7*, 179−192.
(59) Keeling-Tucker, T.; Brennan, J. D. *Chem. Mater.* **2001**, *13*, 3331−3350.
(60) Frenkel-Mullerad, H.; Avnir, D. *J. Am. Chem. Soc.* **2005**, *127*, 8077−8081.
(61) Gulcev, M. D.; Goring, G. L. G.; Rakic, M.; Brennan, J. D. *Anal. Chim. Acta* **2002**, *457*, 47−59.
(62) Monton, M. R. N.; Forsberg, E. M.; Brennan, J. D. *Chem. Mater.* **2011**, *24*, 796−811.
(63) Avnir, D.; Coradin, T.; Lev, O.; Livage, J. *J. Mater. Chem.* **2006**, *16*, 1013−1030.
(64) Brook, M. A.; Chen, Y.; Guo, K.; Zhang, Z.; Brennan, J. D. *J. Mater. Chem.* **2004**, *14*, 1469−1479.
(65) Brook, M. A.; Chen, Y.; Guo, K.; Zhang, Z.; Jin, W.; Deisingh, A.; Cruz-Aguado, J.; Brennan, J. D. *J. Sol-Gel Sci. Technol.* **2004**, *31*, 343−348.
(66) Carrasquilla, C.; Li, Y.; Brennan, J. D. *Anal. Chem.* **2011**, *83*, 957−965.
(67) Besanger, T. R.; Hodgson, R. J.; Guillon, D.; Brennan, J. D. *Anal. Chim. Acta* **2006**, *561*, 107−118.